PCARE and WASF3 regulate ciliary F-actin assembly that is required for the initiation of photoreceptor outer segment disk formation

Julio C. Corral-Serrano[a,b], Ideke J. C. Lamers[a,b,1], Jeroen van Reeuwijk[a,b,1], Lonneke Duijkers[a], Anita D. M. Hoogendoorn[a], Adem Yildirim[c], Nikoleta Argyrou[a,b], Renate A. A. Ruigrok[a], Stef J. F. Letteboer[a], Rossano Butcher[d], Max D. van Essen[a], Sanae Sakami[e], Sylvia E. C. van Beersum[a], Krzysztof Palczewski[e,3], Michael E. Cheetham[f], Qin Liu[d], Karsten Boldt[g], Uwe Wolfrum[c], Marius Ueffing[g], Alejandro Garanto[a,h], Ronald Roepman[a,b,2,3], and Rob W. J. Collin[a,h,2]

[a]Department of Human Genetics, Radboud University Medical Center, 6525 GA, Nijmegen, The Netherlands; [b]Radboud Institute for Molecular Life Sciences, Radboud University Medical Center, 6525 GA, Nijmegen, The Netherlands; [c]Institute of Molecular Physiology, Johannes Gutenberg University of Mainz, 55099 Mainz, Germany; [d]Department of Ophthalmology, Ocular Genomics Institute, Massachusetts Eye and Ear, Harvard Medical School, Boston, MA 02114; [e]Department of Pharmacology, School of Medicine, Case Western Reserve University, Cleveland, OH 44106; [f]UCL Institute of Ophthalmology, University College London, London EC1V 9EL, United Kingdom; [g]Center of Ophthalmology, Institute for Ophthalmic Research, University of Tübingen, 72076 Tübingen, Germany; and [h]Donders Institute for Cognitive Neuroscience, Radboud University Medical Center, 6525 GA, Nijmegen, The Netherlands

Edited by David S. Williams, University of California, Los Angeles, CA, and accepted by Editorial Board Member Jeremy Nathans February 28, 2020 (received for review February 26, 2019)

The outer segments (OS) of rod and cone photoreceptor cells are specialized sensory cilia that contain hundreds of opsin-loaded stacked membrane disks that enable phototransduction. The biogenesis of these disks is initiated at the OS base, but the driving force has been debated. Here, we studied the function of the protein encoded by the photoreceptor-specific gene *C2orf71*, which is mutated in inherited retinal dystrophy (RP54). We demonstrate that C2orf71/PCARE (photoreceptor cilium actin regulator) can interact with the Arp2/3 complex activator WASF3, and efficiently recruits it to the primary cilium. Ectopic coexpression of PCARE and WASF3 in ciliated cells results in the remarkable expansion of the ciliary tip. This process was disrupted by small interfering RNA (siRNA)-based down-regulation of an actin regulator, by pharmacological inhibition of actin polymerization, and by the expression of PCARE harboring a retinal dystrophy-associated missense mutation. Using human retinal organoids and mouse retina, we observed that a similar actin dynamics-driven process is operational at the base of the photoreceptor OS where the PCARE module and actin colocalize, but which is abrogated in *Pcare*$^{-/-}$ mice. The observation that several proteins involved in retinal ciliopathies are translocated to these expansions renders it a potential common denominator in the pathomechanisms of these hereditary disorders. Together, our work suggests that PCARE is an actin-associated protein that interacts with WASF3 to regulate the actin-driven expansion of the ciliary membrane at the initiation of new outer segment disk formation.

photoreceptor | cilium | outer segments | actin | retinitis pigmentosa

Photoreceptor cells in the neural retina of vertebrates are postmitotic, neuroepithelial cells that are highly polarized and compartmentalized (1–3). The apical phototransductive outer segment (OS) resembles a highly modified primary sensory cilium and is connected to the biosynthetic compartment, the inner segment (IS), by a narrow microtubule-based connecting cilium (CC) that is homologous to the transition zone (TZ) of a primary nonmotile cilium (4, 5). The replacement of aged damaged molecular OS components requires renewal by a specialized refurbishing mechanism. Daily, ∼10% of the rod photoreceptor's opsin-loaded disks (6) are shed at the apical OS tip, and phagocytized by the adjacent retinal pigment epithelium (RPE) cells, while the same amount of new membrane disks are generated and restacked at the OS base, ensuring photoreceptor homeostasis. The canonical mechanism behind the onset of the formation of new disks was initially proposed (7) and recently established (8) to be evagination and subsequent expansion of the ciliary plasma membrane at the compartment where the CC enters the OS base. Actin was proposed to be a critical factor in this, after a branched actin network was observed at the site of evagination initiation over three decades ago (9, 10), and inhibition of actin polymerization interfered with this process (11). Despite these observations, detailed molecular insights into the dynamics or regulation of this actin-driven membrane evagination process have remained elusive.

We set out to identify the molecular disease mechanism of a progressive subtype of inherited retinal dystrophy, autosomal recessive retinitis pigmentosa type 54 (RP54) that is caused by

Significance

The photoreceptor outer segments are primary cilia, modified for phototransduction by incorporation of stacked opsin-loaded membrane disks that are continuously regenerated. This process is disrupted in several types of inherited retinal dystrophy, but the driving force remained unclear. We show that C2orf71/PCARE (photoreceptor cilium actin regulator), associated with inherited retinal dystrophy subtype RP54, efficiently recruits the Arp2/3 complex activator WASF3 to the cilium. This activates an actin dynamics-driven expansion of the ciliary tip, resembling membrane evagination in lamellipodia formation. Colocalization of this actin dynamics module to the base of the outer segments, and absence thereof in *Pcare*$^{-/-}$ mice, suggests PCARE-regulated actin dynamics as a critical process in outer segment disk formation.

Author contributions: J.C.C.-S., I.J.C.L., J.v.R., K.P., Q.L., U.W., M.U., R.R., and R.W.J.C. designed research; J.C.C.-S., I.J.C.L., J.v.R., L.D., A.D.M.H., A.Y., N.A., R.A.A.R., S.J.F.L., R.B., M.D.v.E., S.S., S.E.C.v.B., K.B., and A.G. performed research; J.C.C.-S., I.J.C.L., and J.v.R. analyzed data; J.C.C.-S., I.J.C.L., J.v.R., M.E.C., R.R., and R.W.J.C. wrote the paper; and K.P., M.E.C., Q.L., U.W., M.U., A.G., R.R., and R.W.J.C. supervised research.

The authors declare no competing interest.

This article is a PNAS Direct Submission. D.S.W. is a guest editor invited by the Editorial Board.

[1]I.J.C.L. and J.v.R. contributed equally to this work.

[2]R.R. and R.W.J.C. contributed equally to this work.

[3]To whom correspondence may be addressed. Email: ronald.roepman@radboudumc.nl.

This article contains supporting information online at https://www.pnas.org/lookup/suppl/doi:10.1073/pnas.1903125117/-/DCSupplemental.

mutations in *C2orf71* (12, 13). Using an affinity capture approach, we identified a number of proteins potentially interacting with C2orf71, either directly or indirectly. These included basal body/centriole-associated proteins, microtubule-associated proteins, and, intriguingly, also several proteins involved in the nucleation and assembly of actin filaments (F-actin). We have proposed to rename *C2orf71* as *PCARE*, which stands for "photoreceptor cilium actin regulator," as our study indicates that this protein plays an important role in delivering actin-associated components to the base of the photoreceptor OSs to regulate the initial development of OS disks.

Results

PCARE Is a Ciliary and Actin-Associated Protein. *PCARE* is predominantly expressed in the retina (12) and encodes a 140-kDa ciliary protein that is predicted to be myristoylated and palmitoylated at its N terminus (*SI Appendix*, Fig. S1*A*) (13). These posttranslational modifications promote stable attachment to membranes and are critically important in ciliary translocation (14). PCARE does not contain any highly conserved functional domains, but several structural protein sequence motifs are predicted, including a tentative actin-binding motif (*SI Appendix*, Fig. S1*A*). Evaluation of the localization of full-length and three subfragments (*SI Appendix*, Fig. S1*A*) of PCARE in ciliated human telomerase reverse transcriptase immortalized RPE cells (hTERT RPE1) (*SI Appendix*, Fig. S2*A*) showed that both full-length PCARE and the N-terminal fragment 1 (PCARE-F1; amino acids [aa] 2 to 449) localize to the basal body and axoneme of the primary cilium. The middle fragment 2 (PCARE-F2; aa 450 to 900) localizes to the cytosol, where it appears to induce and/or decorate cellular cytoskeletal filaments. Costaining with fluorescent phalloidin indicated that these filaments are actin-based (*SI Appendix*, Fig. S2*B*). The C-terminal fragment 3 (PCARE-F3; aa 901 to 1,289) that contains a predicted nuclear localization signal mainly localizes to the nucleus, although some axonemal staining was also observed (*SI Appendix*, Fig. S2*A*).

PCARE Interacts with Microtubule-, Centrosome-, and Actin-Associated Proteins. We used PCARE as a bait in protein–protein interaction screens to identify potential physical links to known biochemical pathways. Screens for binary retinal interactors of PCARE and its three subfragments were carried out using the yeast two-hybrid (Y2H) system (*SI Appendix*, Table S1). Assessment of the resulting 41 candidate interactors revealed six proteins that are known to be associated with the centriole(s) of the centrosome and/or the ciliary basal body, of which three are known to be involved in retinal ciliopathies, that is, OFD1, CEP290, and CEP250 (15). Other interacting proteins are also microtubule-associated, like the dynactin subunits DCTN1/p150-glued and DCTN2/p50 dynamitin, PCM1, NINL, and KNSTRN. In addition, three components of microtubule-based kinesin motors (KIF20A, KLC2, and KLC4) were found to be associated with PCARE. Importantly, an interaction with one of the key proteins involved in activating actin dynamics was identified, the WAVE regulatory complex (WRC) member WAVE3/WASF3 (Wiskott-Aldrich syndrome protein family member 3) (16). The WRC binds to and, upon activation by, for example, Rac GTPase (17), promotes actin nucleating activity of the ubiquitous ARP2/3 complex, thereby driving the formation of a dynamic branched F-actin network (18). Next to WASF3, five other proteins with different roles in actin dynamics were identified as putative PCARE interactors (*SI Appendix*, Fig. S1*B* and Table S1). For WASF3,

Table 1. Proteins identified in mass spectrometry (TAP) and Y2H experiments with PCARE

Gene symbol	PCARE_Y2H_prey	count	PCARE_TAP_exp	count	Gene symbol	PCARE_Y2H_prey	count	PCARE_TAP_exp	count
WASF3	8		3		OGFOD3	ND		4	
*DCTN2**	1		2		PITRM1	ND		4	
*PCM1**	9		1		UFM1	ND		4	
IFFO1	2		1		**VASP**	ND		4	
KIF20A	2		1		ABCB10	ND		3	
CDR2*	89		ND		ABHD12	ND		2	
FILIP1L	11		ND		**ACTR3B**	ND		2	
AKAP9	10		ND		**ARPC1A**	ND		2	
ANKHD1	6		ND		**ARPC1B**	ND		2	
*DCTN1**	3		ND		**ARPC2**	ND		2	
ACTN1	2		ND		**ARPC4**	ND		2	
CCDC150	2		ND		BAG3	ND		2	
CEP295	2		ND		BAG4	ND		2	
EMILIN3	2		ND		CS	ND		2	
GOLGA3	2		ND		ELL	ND		2	
IL4I1	2		ND		FBXO17	ND		2	
KANSL1	2		ND		FBXW11	ND		2	
*NINL**	2		ND		GALNT2	ND		2	
SPTBN2	2		ND		HSD17B10	ND		2	
SPTBN5	2		ND		LCLAT1	ND		2	
TAX1BP1	2		ND		NIPSNDPA	ND		2	
ENAH	ND		5		**PFN2**	ND		2	
ACTR3	ND		4		PIP4K2C	ND		2	
ARPC3	ND		4		**PPP1R9B**	ND		2	
					SRPRA	ND		2	

Proteins shown were identified in PCARE TAP and Y2H, or in Y2H only, with ≥2 clones, or identified in ≤5 similar TAP experiments from a total of 217 different bait proteins (43). Bold denotes proteins associated to actin dynamics; italics denote proteins associated to microtubules; ND, not detected.

*Potentially nonspecific positives in Y2H library screens, based on common affinity to unrelated baits in 50 in-house Y2H experiments.

two-directional coimmunoprecipitation experiments revealed that the main interacting region was delineated to the N-terminal PCARE F1, while PCARE F2 also had some residual binding of this protein (*SI Appendix*, Fig. S2 *C* and *D*). These fragments also colocalized with WASF3 (*SI Appendix*, Fig. S2*E*).

To further explore the PCARE interactome, we performed tandem affinity purification (TAP) of Strep-II/FLAG tagged full-length PCARE expressed in HEK293T cells. Potentially interacting proteins were subsequently identified by mass spectrometry (MS) (Dataset S1). Although limited overlap is generally observed in Y2H and TAP MS data (19), five proteins, DCTN2, KIF20A, IFFO1, PCM1, and WASF3, were found to potentially interact with PCARE in both the Y2H and the TAP assay (Table 1). Moreover, the three functional protein modules we identified by the Y2H assays could also be distinguished in this experiment: a microtubule-associated module (7 proteins), a centrosome/basal body module (12 proteins), and 18 proteins that are known to play diverse roles in de novo F-actin network assembly. This actin module includes most members of the ARP2/3 complex that initiates actin polymerization, namely, the actin assembly regulator ENAH, the actin capping/severing protein gelsolin, the actin cytoskeleton restructuring factors profilin 1 and 2, myosin regulatory subunits 12A and 12B, the actin bundling protein LIMA1, the actin bundling and membrane-associating protein filamin A, and several chaperonins (*SI Appendix*, Fig. S1*B* and Dataset S1).

PCARE Colocalizes with Actin-Associated Proteins at the OS Base. Given the strong link between PCARE and WASF3, we next evaluated their localization within the retina. Immunofluorescence staining of PCARE and its interactors WASF3 and α-actinin (ACTN1) in human retina showed staining in the area of the CC (Fig. 1). Costaining with centrin-3 that marks the axoneme of the CC and the daughter centriole showed that all three proteins localized at the site of initiation of OS disk morphogenesis in the apical CC region of photoreceptors, where F-actin colocalized with WASF3. The three proteins (PCARE, WASF3, and ACTN1) also localized to the base of the CC and the daughter centriole (Fig. 1). Evaluation of the actin dynamics module in retinae of 1-mo-old *Pcare*$^{-/-}$ mice that develop early-onset retinal degeneration (20) showed that the expression of WASF3 and F-actin within the CC region was reduced when compared to that of wild-type (WT) retinae, while the CC itself remained present, as indicated by the staining of the axonemal marker polyglutamylated tubulin (GT335) (Fig. 2 *A*–*C*). To validate the localization of PCARE within mouse photoreceptor cells, a construct encoding human PCARE was injected and electroporated into neonatal mice. Subsequent analysis confirmed the expression of PCARE at the base of the OS disks, although no obvious staining at the basal body was observed (Fig. 2*D*). Unfortunately, the antibody directed against human PCARE that we generated, as well as the one previously used by Kevany et al. (20), does not seem to effectively recognize endogenous mouse PCARE, at least not in conventional immunohistochemistry or Western blot analysis (*SI Appendix*, Fig. S3). In contrast, the antibody did show a clear and specific signal in immuno-electron microscopy (immuno-EM) which further validated and specified our findings (Fig. 2 *E* and *F* and *SI Appendix*, Fig. S3). High-resolution localization analysis of PCARE in mouse photoreceptors revealed that PCARE decorates the microtubules of the apical region of the CC, and extends to the first nascent disks of the OS base (Fig. 2*E*). Furthermore, it localizes to the ciliary basal body (Fig. 2*E*′) and the daughter centriole (Fig. 2*E*), while some more dispersed signal around the basal body and in the IS could also be observed (Fig. 2*E*″). This signal was completely absent from *Pcare*$^{-/-}$ mice, in addition to a more general absence of properly stacked OS disks and disrupted ISs (Fig. 2*F*). Additional immuno-EM images, from sections stained with either the homemade PCARE antibody or the one previously used by Kevany et al. (20), showed a consistent staining at these different locations (*SI Appendix*, Fig. S4 *A* and *B*, quantified in *SI Appendix*, Fig. S4*D*), while, again, no signal was detectable in ultrathin sections of all 27 photoreceptors analyzed from *Pcare*$^{-/-}$ mice (*SI Appendix*, Fig. S4*C*).

PCARE Recruits WASF3 to the Ciliary Tip and Induces Membrane Expansion. To further study the importance of our findings, we first evaluated the localization of ectopically expressed PCARE and several of its putative interactors. For the majority of them, their intracellular localization in ciliated hTERT RPE1 cells did not obviously change upon coexpression of PCARE (*SI Appendix*, Fig. S5). ARP3 and SPATA7, however, as well as the TZ marker RPGRIP1L, were also detected along the ciliary axoneme after coexpression with PCARE (*SI Appendix*, Fig. S5). Interestingly, the localization changed dramatically for the ARP2/3 complex activating factor WASF3 (Fig. 3 *A*–*G*). In the absence of PCARE, which is not endogenously expressed in these cells, WASF3 associates to F-actin in the vicinity of the nucleus, and not in the cilium (Fig. 3 *C* and *D*). When PCARE was coexpressed, however, it efficiently recruited WASF3 and translocated it into the cilium (Fig. 3 *E* and *F*), where actin filaments could be identified (Fig. 3*F*). Intriguingly, this induced the formation of a ciliary membrane expansion, with some variation in shape and size (Fig. 3 *E*′ and *F*′). This process was not cell-type specific, as it could also be detected in murine ciliated

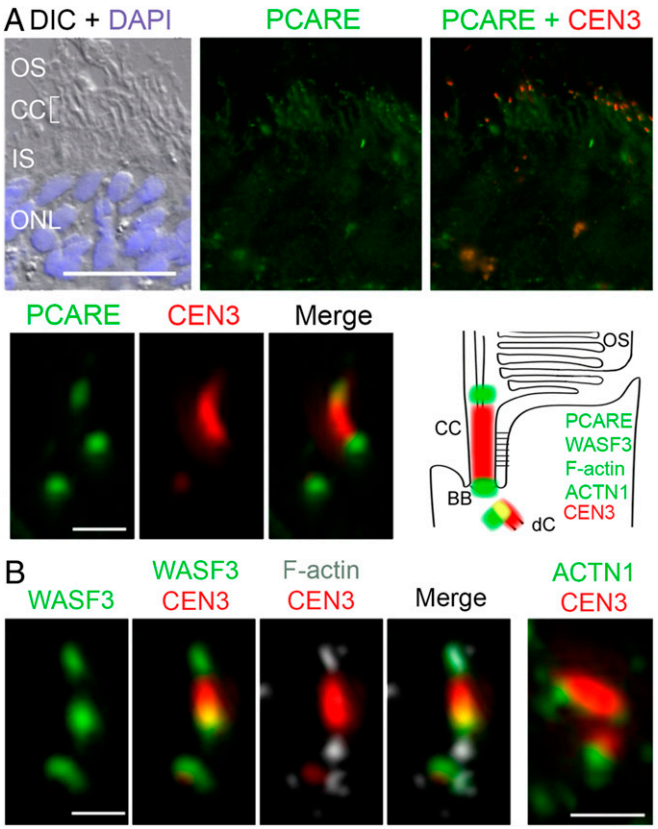

Fig. 1. PCARE colocalizes with actin-associated proteins at the base of photoreceptor OSs. Localization of PCARE, WASF3, ACTN1, and F-actin in a human donor retina. (*A*) PCARE localizes at the tip of the CC, counterstained with anti-centrin-3 (CEN3), at the basal body (BB) and the adjacent daughter centriole (dC). (*B*) The same localization pattern is observed for the actin-associated proteins WASF3, ACTN1, and F-actin, which is summarized in the schematic diagram of the corresponding area of a rod photoreceptor. (Scale bars: [*A*] *Upper*, 25 μm, and *Lower*, 1 μm; [*B*] 1 μm.)

IMCD3 cells (*SI Appendix*, Fig. S6). Several intermediate stages of this process could be observed, suggesting a progressive expansion over time at the ciliary tip (Fig. 3 *E*–*G*). A more detailed evaluation of several confocal planes of a cell ectopically coexpressing PCARE, WASF3, and the centrosomal/basal body protein DCTN2, another potential PCARE interactor, further demonstrated that docking of the module at the ciliary tip initiates the ciliary membrane expansion (*SI Appendix*, Fig. S7). Finally, to study the localization of endogenous PCARE and WASF3 in the developing human photoreceptor cells, induced pluripotent stem cell (iPSC) technology was applied. Stem cells derived from a healthy individual were differentiated toward three-dimensional retinal organoids, and stained for PCARE and WASF3 at different stages during development. As shown in Fig. 3*H*, both proteins appear to be present at the developing photoreceptor cilium at 120 days of differentiation. From day 150 onward, the expression became more apparent at the tip of the cilium, and expansions of the tip started to appear. This was even more evident at day 180 of differentiation, where both PCARE and WASF3 were found to be present at these expansions. Together, our data suggest that PCARE and WASF3 cooperate in the remodeling of ciliary membranes, not only in transfected cells but also in cells with endogenous expression levels of all components participating in this process, as shown in the developing retinal organoids.

Actin- and Tubulin-Associated Proteins Localize to the Ciliary Tip Expansions. Evaluation of the constitution of the expansions in ciliated hTERT RPE1 cells by immunofluorescence showed that they contain all tested core components of the potential

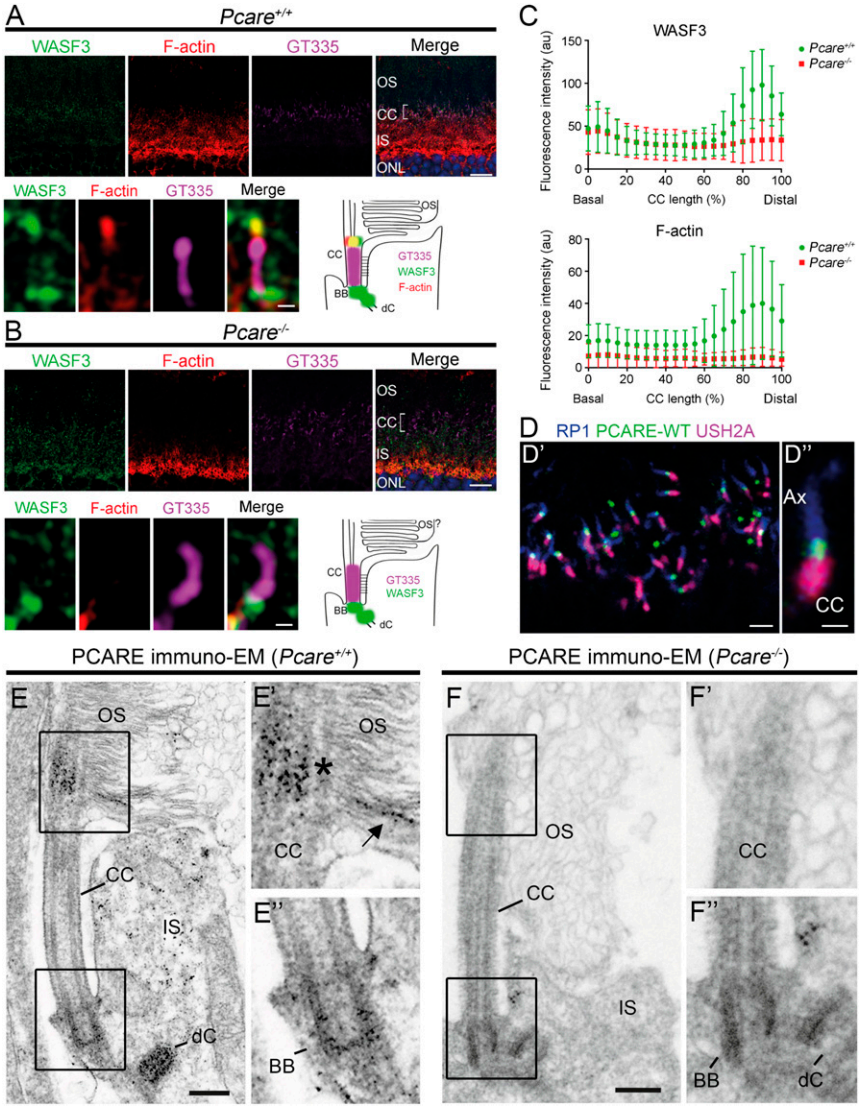

Fig. 2. *Pcare*$^{-/-}$ photoreceptors show mislocalization of WASF3 and F-actin, disorganized OS disk membranes, and reduced ISs. (*A* and *B*) In *Pcare*$^{-/-}$ mouse retinas, WASF3 and F-actin show a reduced expression and mislocalize from the distal part of the CC. The schematic diagrams show the corresponding areas of rod photoreceptors. (*C*) Quantification of WASF3 and F-actin expression in WT or *Pcare*$^{-/-}$ mice along the CC from the basal to the distal part. (*D* and *D*′) Localization of WT NTAP-PCARE in mouse photoreceptor cells following in vivo electroporation, visualized at (*D*) low resolution and (*D*′) high resolution. FLAG-tagged WT PCARE (green) is localized to the junction between the Rp1-labeled axoneme (Ax, blue) and the Ush2A-labeled CC region (purple). (*E* and *F*) Immuno-EM localization of PCARE in *Pcare*$^{+/+}$ and *Pcare*$^{-/-}$ mouse photoreceptors. (*E*, *E*′, and *E*″) In WT animals, PCARE localizes to the photoreceptor OS at the tip of the CC (asterisks) associated with nascent disks (arrows) and the centrioles of photoreceptors. (*F*, *F*′, and *F*″) The prominent labeling of the OS base in *C* is absent in *Pcare*$^{-/-}$ photoreceptors. (Scale bars: [*A* and *B*] Upper, 10 μm, and *Lower*: 0.5 μm; [*E*] 300 nm; [*D* and *D*′] 2 μm; [*D*″] 0.5 μm; [*E*′ and *E*″] 150 nm; [*F*] 300 nm; [*F*′ and *F*″] 150 nm.) All animals were 1 mo old. ONL, outer nuclear layer.

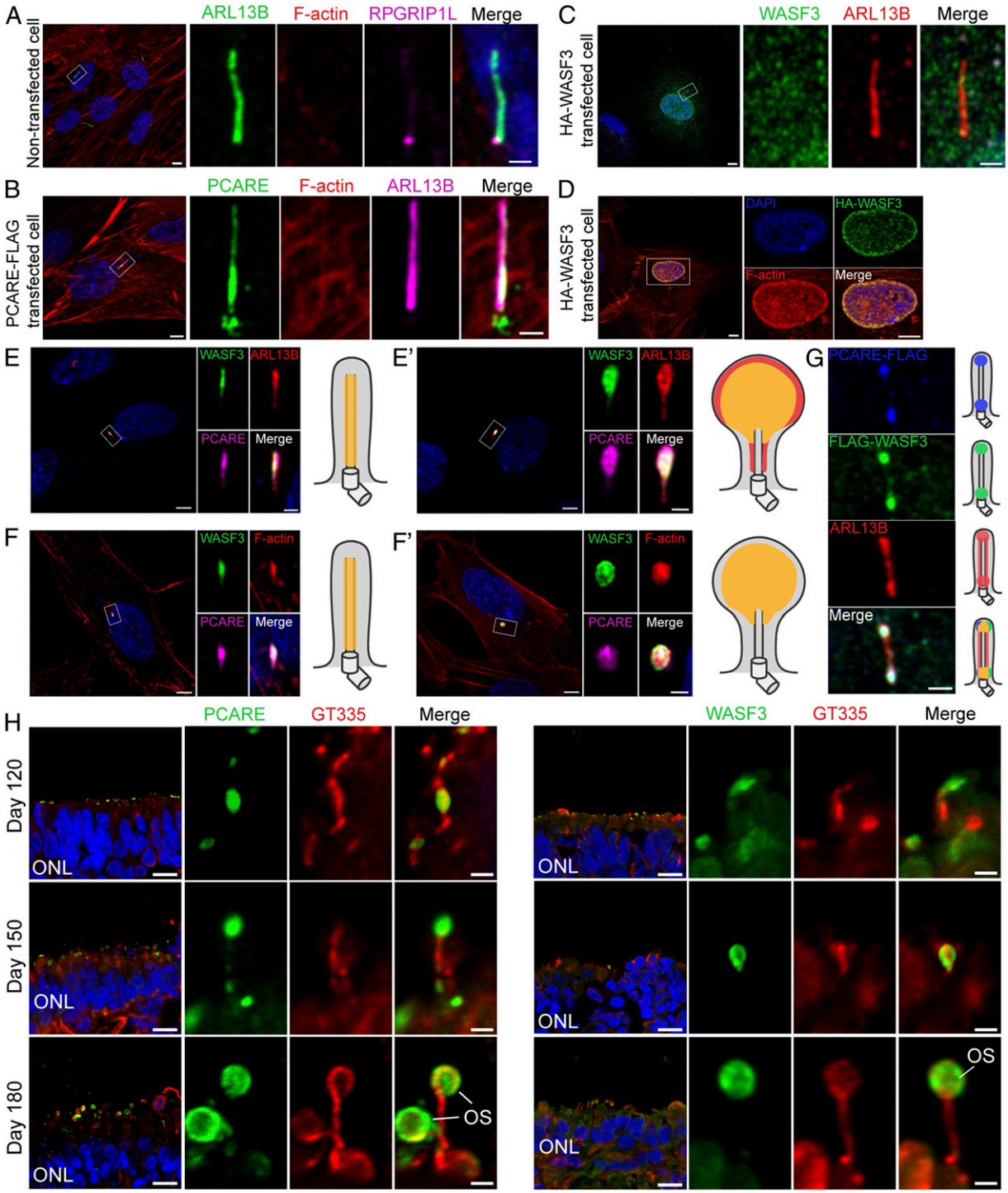

Fig. 3. Formation of ciliary expansions upon ectopic coexpression of PCARE and WASF3, as well as in retinal organoids. (*A*) The primary cilium of a non-transfected hTERT RPE-1 cell stained with an antibody against F-actin demonstrates absence of polymerized actin along the ciliary axoneme. (*B*) Ectopic expression of PCARE in hTERT RPE1 cells shows localization of PCARE (green) at both the ciliary base and axoneme, and faint presence of F-actin (red) inside the primary cilium, stained with ARL13B (purple). (*C*) Ectopically expressed WASF3 is absent from the primary cilium, and (*D*) localizes to the cell nucleus, where it recruits F-actin. (*E*) Coexpression of PCARE-FLAG and HA-WASF3 generates translocation of the latter from the nucleus into the cilium. (*E′*) An expansion or bulging of the ciliary plasma membrane was observed in a number of PCARE-FLAG and HA-WASF3 double transfected cells. (*F* and *F′*) Double transfected cells with PCARE-FLAG and HA-WASF3 strongly recruit F-actin into normal and expanded cilia (*Left*). Schematic diagrams illustrate the observed localizations (overlap of all colors indicated in orange) (*Right*). (*G*) Cells were transfected with plasmids expressing FLAG-WASF3 and PCARE-FLAG and stained 4 h after transfection with antibodies directed against ARL13B (red), WASF3 (green), and PCARE (blue). At this point, there is accumulation of the proteins PCARE and WASF3 at the ciliary base and tip. (*E-G*) Schematic diagrams of cilia (*Right*) illustrate the observed localizations (overlap of all colors indicated in orange). (*H*) Human iPSCs were differentiated into retinal organoids, fixed, and cryopreserved at day 120, 150, or 180. Cryosections were stained with antibodies directed against polyglutamylated tubulin (GT335, red) to mark the photoreceptor cilium, and PCARE (*Left*) or WASF3 (*Right*). PCARE and WASF3 form a ring structure on the axoneme and tip of the photoreceptor cilium, which evaginates at day 180 to start forming OSs. (Scale bars: 10 μm [*Left*]; 5 μm [other images].)

PCARE-associated actin dynamics module we identified in our affinity screens: ENA/VASP (*SI Appendix*, Fig. S8*A*) and the Rho GEF kinase kalirin (*SI Appendix*, Fig. S8*B*), that is known to affect the actin cytoskeleton and is a RAC1 activator (21). RAC1 was not identified in our affinity screen but is known to activate the WRC (22), and was also present at the expansions (*SI Appendix*, Fig. S8*C*). Coexpression of PCARE, WASF3, and the ARP3 protein, a member of the ARP2/3 complex and involved in activation of the branched F-actin network (23), did confirm colocalization of these proteins and F-actin throughout the expansion (*SI Appendix*, Fig. S8*D*). Evaluation of the localization of markers of the ciliary microtubule axoneme, acetylated tubulin (*SI Appendix*, Fig. S9*A*), and polyglutamylated tubulin (*SI Appendix*, Fig. S9*B*) upon ectopic coexpression of PCARE and WASF3 showed a partial colocalization, which was also the case for the intraflagellar transport protein IFT88 (*SI Appendix*, Fig. S9*C*) and lebercilin/LCA5 (*SI Appendix*, Fig. S9*D*).

Distinct Retinal Ciliopathy Proteins Modify the Structure of the Ciliary Expansions. Interestingly, we observed that the ciliary marker ARL13B (Fig. 3 *A*–*F*) and the ciliary TZ marker RPGRIP1L (*SI Appendix*, Fig. S8 *B* and *C*) also localized to the expansions. Mutations in these two proteins cause the retinal ciliopathy Joubert syndrome, and genes encoding several of the other identified putative PCARE interactors have also been found to be mutated in ciliopathies. Upon ectopic coexpression of PCARE and WASF3, we identified that several of these proteins are cotranslocated into the ciliary tip expansions, similar to RPGRIP1L and ARL13B. These include the basal body protein OFD1 (*SI Appendix*, Fig. S10*B*) and the proteins SPATA7 (*SI Appendix*, Fig. S10*C*) and lebercilin/LCA5 (*SI Appendix*, Fig. S9*D*) that normally localize to the ciliary compartment. Two potential PCARE interactors of the centrosomal/basal body module that we tested, DCTN2 (*SI Appendix*, Fig. S7*A*) and CEP250 (*SI Appendix*, Fig. S7*B*), however, were not translocated to the ciliary expansions and remained at the ciliary basal body. Not only were OFD1 and SPATA7 efficiently translocated to the expansion structures, their coexpression also further increased their size, on average, 40%, compared to those found when overexpressing only PCARE and WASF3 (*SI Appendix*, Fig. S10).

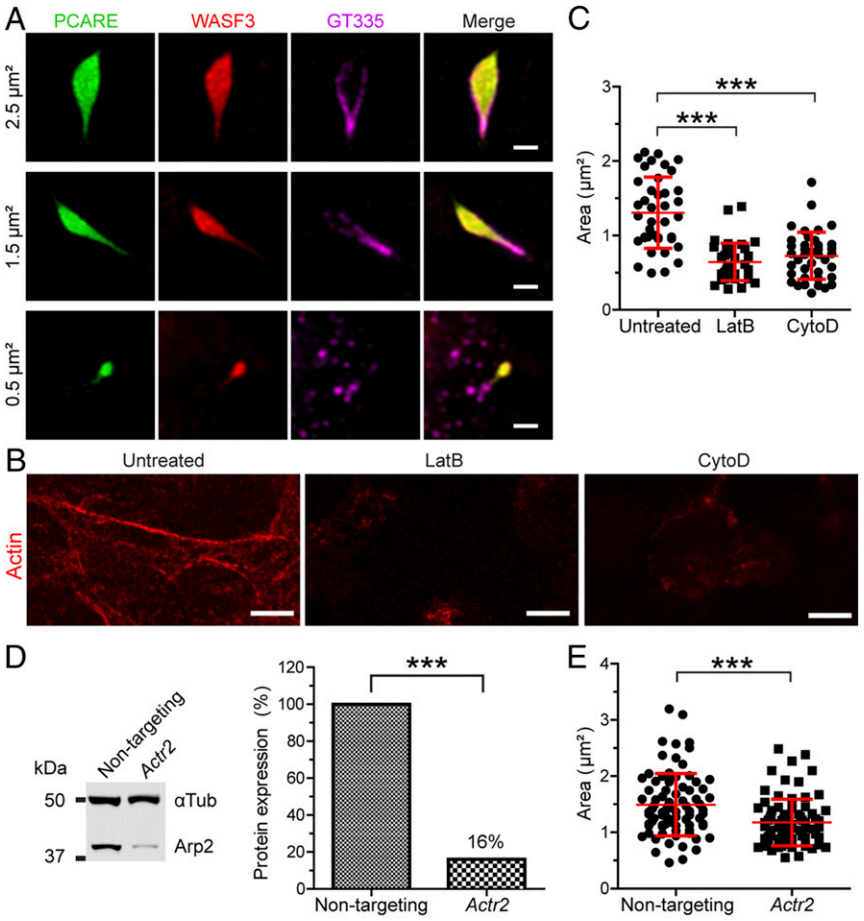

Fig. 4. The size of PCARE and WASF3-mediated ciliary expansions is decreased by actin poisons and knockdown of Arp2. (*A*) Representative images of three different sizes of ciliary expansions in ciliated stable IMCD3-PCARE cells transfected with 3xHA-WASF3. Cells are stained with antibodies directed against PCARE (green), WASF3 (red), and GT335 (purple, ciliary marker). (*B*) Representative images of phalloidin staining in stable IMCD3-PCARE cells transfected with 3xHA-WASF3 that were either untreated or treated with 1 µM Cytochalasin D (CytoD) or 1 µM Latrunculin B (LatB). Phalloidin staining (red) is used as a positive control in order to evaluate the efficiency of the actin poisons. (*C*) Quantification of the area of the WASF3 signal as a measure of expansion size is represented for each cilium per condition, and revealed a statistically significant decrease in size for cells treated with CytoD and LatB (untreated vs. LatB: ***P value < 0.0001, $n = 40$; for untreated vs. CytoD: ***P value < 0.0001, $n = 40$). The mean and SD of each condition is indicated in red. (*D*) Western blot (*Left*) and graph (*Right*) of Arp2 expression in IMCD3 cells transfected with nontargeting or *Actr2* siRNA pools. A significant decrease in Arp2 expression was observed after *Actr2* knockdown (***P value < 0.0001). (*E*) Evaluation of the area of the WASF3 signal as a measure of ciliary expansion size in cells treated with siRNA pools shows a significant decrease in expansion size in *Actr2* knockdown cells (nontargeting vs. *Actr2*: ***P value < 0.0001, $n = 80$). The mean and SD of each condition is indicated in red. (Scale bar: [*A*] 1 µm; [*B*] 5 µm.)

Inhibition of Actin Remodeling Pathways Affects the Expansion Formation. To better quantify the degree of membrane expansions in ciliated cells, a stable IMCD3 cell line expressing WT PCARE was generated using the Flp-In system (24). Ciliary localization of PCARE, similar to that observed upon single transfection of hTERT RPE1 cells (Fig. 3*B* and *SI Appendix*, Fig. S11), as well as the ability to form expansions upon transient expression of WASF3 in these cells, was confirmed via immunocytochemistry. The size of these expansions varied between cells, most probably due to the different degree of WASF3 expression following transient transfection (Fig. 4*A* and *SI Appendix*, Fig. S12). Subsequently, we employed this stable cell line to validate that actin dynamics are involved in the formation of these expansions. For this, we treated the cells with two actin polymerization inhibitors, namely, cytochalasin D, which prevents polymerization of the barbed/plus ends of actin filaments (25), and latrunculin B, which sequesters G-actin monomers and thereby prevents its polymerization (26). Using a treatment regime (in terms of time and concentration) that did not affect general cellular processes, but did show a loss of actin polymerization (Fig. 4*B*), transient coexpression of WASF3 together with either of the two compounds resulted in a significant reduction of expansion size (Fig. 4*C*). In addition, we also studied whether down-regulation of one of the components driving the nucleation of actin would affect the formation of the expansions. Treatment of the stable IMCD3 cell line with small interfering RNA (siRNA) targeting *Actr2* (the mouse ortholog of *ARP2*) resulted in a reduction of more than 80% of ARP2 protein (Fig. 4*D*). When comparing the size of the expansions formed following transient expression of WASF3 combined with either nontargeting siRNAs or the ones targeting *Arp2*, again, a clear reduction in the average size of the expansions was observed following knock-down of *Arp2* (Fig. 4*E*). The fact that the reduction in size was less prominent compared to that observed using the pharmacological inhibitors is most likely explained by the residual *Arp2* expression.

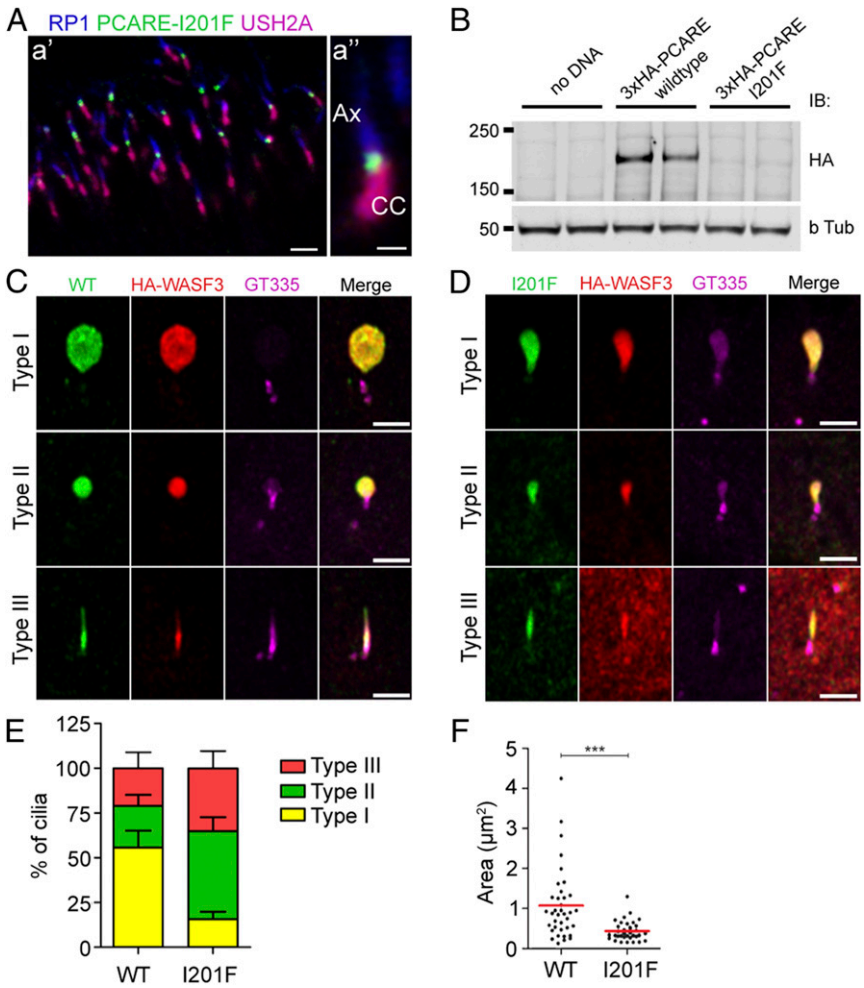

Fig. 5. RP-associated PCARE missense mutation p.(I201F) impairs ciliary expansion. (*A* and *A′*) Localization of p.(I201F) mutant NTAP-PCARE (PCARE-I201F) in mouse photoreceptor cells following in vivo electroporation, visualized at (*A*) low-resolution (*A*) and (*A′*) high resolution. FLAG-tagged mutant PCARE (green) is localized to the junction between the Rp1-labeled axoneme (Ax, blue) and the Ush2A-labeled CC (purple). (*B–F*) The hTERT RPE1 cells were cotransfected with plasmids expressing FLAG-tagged WASF3, and either WT PCARE or p.(I201F) mutant PCARE fused to HA. (*B*) Western blot analysis of cell lysates transfected with HA-tagged WT or mutant PCARE, stained with anti-HA antibody (*Upper*). Tubulin was stained for normalization purposes (*Lower*). (*C* and *D*) Cells were stained with antibodies recognizing PCARE (green), WASF3 (red), and polyglutamylated tubulin (GT335, purple). To compare the cilia transfected with WT PCARE (WT) to mutant PCARE (I201F), we categorized the different phenotypes in type I (extensive ciliary tip expansion), II (small expanded tip), or III (regular cilium, no obvious expansion) structures. (*E*) Cells transfected with mutant PCARE contain more type III cilia than WT transfected cells. (*F*) Quantification of the area of the expansions is represented for each measured cilium, and shows that cells transfected with the I201F mutant present cilia with smaller expansion areas than the WT: ($n = 37$), p.I201F ($n = 34$), ***P value < 0.0001. (Scale bars: [*A′*] 2 μm; [*A″*] 0.5 μm; [*C* and *D*] 2 μm.)

Mutant p.(I201F) PCARE Alters the Formation of Expansions. To investigate the pathophysiology underlying *PCARE*-associated RP54, the p.(I201F) missense mutation (13) was introduced into PCARE. First, a construct encoding p.(I201F) mutant PCARE was injected and electroporated into neonatal mice. Similar to the expression of WT PCARE (Fig. 2*D*), p.(I201F) mutant PCARE was localized at the base of the OS in mouse photoreceptor cells (Fig. 5*A*), suggesting that this mutant protein can still be translocated to its proper location. To study the ability of p.(I201F) mutant PCARE to form ciliary membrane expansions, hTERT RPE1 cells were transfected with either WT or p.(I201F) mutant PCARE. Western blot analysis revealed that, in agreement with previous results (13), the p.(I201F) mutant PCARE protein appears to be less stable compared to the WT protein (Fig. 5*B*). Coexpression of WT or mutant PCARE with WASF3 showed that, although p.(I201F) mutant PCARE still translocated to the ciliary axoneme, there were clear differences in the size and the number of expansions formed by WT vs. mutant PCARE (Fig. 5 *C*–*F*), most probably due to the reduced levels of the unstable mutant protein. To analyze these differences in more detail, we classified the different cilia phenotypes of cotransfected cells into three types: type I (large, extended expansion), type II (small expansion), and type III (no expansion) (Fig. 5 *C* and *D*). Three independent evaluations of these cilia were performed in a total of 40 cilia for the WT condition and 41 cilia for the mutant condition (Fig. 5*E*). The majority of the cilia (~79% of the total for the WT and ~65% for the mutant) presented some degree of expansion. Importantly, cells transfected with WT PCARE contained predominantly cilia with the large, extended expansions (type I, 56% on average) compared to the PCARE p.(I201F) mutant (16% on average). Moreover, the area of the expansions was significantly reduced when mutant PCARE was expressed, compared to the WT (Fig. 5*F*).

Discussion

The combination of high-resolution imaging studies with protein–protein interaction analyses has been shown to be an effective way to expand our knowledge of cilium function in health and disease in an iterative way (5, 27, 28). In this study, we took this approach of investigating the role of PCARE in the photoreceptor cilium to understand the disease pathogenesis of RP54. Although PCARE is expressed specifically in the retina (12, 20), the full-length protein efficiently localizes to the cilium upon ectopic expression in cultured ciliated cells (i.e., hTERT RPE-1 and IMCD3 cells). PCARE-F1 efficiently localized to the entire cilium including the basal body, similar to the full-length protein, which is likely to be regulated by the predicted N-myristoylation (Gly2) and S-palmitoylation (Cys3) signals present in this fragment. C-terminal PCARE-F3 seems to use its predicted nuclear localization signal to translocate to the nucleus, although the relevance of this signal in full-length PCARE is unclear. Interestingly, PCARE-F2 contains a predicted actin-binding motif, and is indeed capable of decorating actin filaments. This matches our protein–protein interaction data: Besides the identification of several centrosomal/basal body- and microtubule-associated potentially interacting proteins that are in line with the ciliary localization of PCARE, our Y2H screen for binary PCARE interactors yielded several proteins that have been shown to be involved in the regulation of the actin cytoskeleton. This process concerns the dynamic cycling between polymerization and disassembly of the 42-kDa monomeric, globular actin (G-actin) protein into filamentous actin (F-actin), and the subsequent formation of higher-order, branched F-actin networks. This facilitates most cellular processes that require cell membrane protrusion, contraction, and remodeling (29, 30). Most interestingly, we identified WASF3/WAVE3 as a putative PCARE interactor. This protein is incorporated into a conserved, heteropentameric WRC that activates the Arp2/3 complex for actin filament nucleation and assembly of a branched F-actin network (16). The WRC is known to activate the Arp2/3 complex specifically in lamellipodia, ribbon-like flat cell membrane protrusions driven by actin dynamics that provide cellular motility across a surface (31). In turn, the Arp2/3 complex activation occurs downstream of the Rho GTPase family member Rac1. Interestingly, Rac1 can be activated by the Rho GEF kalirin. Both kalirin and α-actinin, identified as prey in the PCARE Y2H screen, are proteins with spectrin-like repeats that allow the interaction with a variety of substrates (32). The association of PCARE with an extensive actin dynamics module was further solidified and extended by our TAP experiments, identifying a further 18 proteins associated with actin dynamics. These included most members of the Arp2/3 complex (that can be activated by WASF3), the actin assembly regulator ENAH, and the actin capping/severing protein gelsolin.

As several differentially localized actin-based processes have been suggested to regulate photoreceptor OS neogenesis and homeostasis (33), it was important to accurately determine the location of PCARE in the retina. As its capacity to localize to the primary cilia of cultured cells already suggested, PCARE was indeed found at the photoreceptor CC. More precise localization by immuno-EM determined that PCARE localizes to three prominent sites: the ciliary basal body, the accompanying daughter centriole, and a narrow region at the tip of the CC stalk, directly adjacent to the site of the neogenesis of the first OS membrane disks. Of note is that some differences in the PCARE localization were observed when employing different methods and species. In particular, the homemade antibody directed against human PCARE did not work in conventional light microscopy of mouse retinal sections, despite the fact that immuno-EM labeling of mouse retinal sections did show a specific localization, that was identical with an anti-PCARE antibody that was previously published (20). To check the localization of ectopically expressed PCARE in mouse retina, an antibody directed against the FLAG-tag was used, only revealing staining at the tip but not at the base of the CC, nor in the IS. This difference with the localization of endogenous PCARE may be caused by the fact that different antibodies were used, or due to other experimental variations that would require further investigations. Similar to PCARE, WASF3 also localized to the three sites around the CC, while F-actin colocalized with WASF3 at its tip. This latter finding was particularly exciting, as it directly links to one of the axioms in photoreceptor cell biology: the observation of a branched F-actin network at this exact location over 30 years ago, when the involvement of F-actin in the neogenesis of OS disks was first suggested (9). This hypothesis was later strengthened by results of treatment with the actin drug cytochalasin D that prohibited the generation of new disks, but not the (over)growth of existing ones (11), and by immuno-EM observations that demonstrated the presence of α-actinin at this site (10). We here demonstrate that ectopic coexpression of PCARE and WASF3 in cultured ciliated cells, in which PCARE is not endogenously expressed, efficiently recruits WASF3 from the cytoplasm to the cilium, where it activates the dynamic formation of an F-actin network that drives membrane expansion, which causes expansion of the ciliary tip. In addition, both proteins colocalized in developing OSs, appearing as ciliary membrane expansions at the tip of the CC stalk in human iPSC-derived retinal organoid cultures (Fig. 3*H*). These were remarkably similar to the ciliary membrane expansions induced by coexpression of PCARE and WASF3, supporting the biological relevance of our model. The fact that the formation of these expansions can be inhibited by the F-actin poisons latrunculin B and cytochalasin D (Fig. 4*C*) confirms the involvement of actin in this process. This was further corroborated by our findings using siRNA-mediated downregulation of Arp2 expression (Fig. 4*E*), one of the proteins involved in actin nucleation. Evaluation of other components

present in these ciliary membrane expansions, either by colocalization or coexpression, confirmed that they contained all tested proteins of the actin dynamics module that were identified in our protein–protein interaction studies (Fig. 6). The translocation of variable levels of polyglutamylated tubulin, as well as acetylated tubulin, to the expansions was also observed (Fig. 3 and *SI Appendix*, Fig. S9), which may indicate a coupling of (stabilized) microtubules to actin dynamics at the distal microtubule plus-ends of the axoneme, analogous to processes at the growth cone periphery (34).

Several aspects of our study provide important insights into the molecular disease mechanisms underlying the disturbed photoreceptor function observed in not only *PCARE*-associated RP but also in several other retinal ciliopathies. First, as we identified that a missense mutation (p.I201F) in PCARE impairs the ciliary tip expansions, we propose that the disturbance of actin dynamics-driven OS disk neogenesis is the underlying mechanism in *PCARE*-associated retinal dystrophy. Both the phenotype of *Pcare*$^{-/-}$ mice (20) and the absence of WASF3 and F-actin observed at the tip of the CC stalk of the photoreceptors in these mice support this hypothesis. Second, *WASF3* variants were identified in a patient with cone–rod dystrophy following whole-genome sequencing (35). As WASF3 is an interactor of PCARE, our data suggest *WASF3* could be a bona fide retinal disease gene. Third, several ciliopathy-associated proteins were translocated to the ciliary tip expansions upon ectopic coexpression of PCARE and WASF3. These proteins include IFT88, RPGRIP1L, ARL13B, SPATA7, and Lebercilin/LCA5. Interestingly, the coexpression of OFD1 and SPATA7 significantly expanded the size of the structures, suggesting a dynamic participation of these proteins in the expansion process. RPGRIP1L was the only protein that clearly translocated from the ciliary TZ to the ciliary compartment only by PCARE without expression of WASF3 (*SI Appendix*, Fig. S5). Finally, the previous detection of both RPGRIP1L and Lebercilin/LCA5 at the apical CC region of mouse photoreceptors by immuno-EM (36, 37), and the recent discovery of the interaction of the X-linked RP-associated protein RPGR with gelsolin (38) (which was also present in our TAP dataset), strengthens the hypothesis that several retinal ciliopathy proteins play a role in the actin-driven ciliary tip expansions. Importantly, focused apical actin dynamics was recently shown to be the driving force of the excision of ciliary tips to precede cilium disassembly (39), and of scission of ectosomes containing potentially functional signaling molecules (40). The latter process was also suggested to be conserved and amplified in photoreceptors to drive OS disk assembly, in close concert with peripherin to regulate upstream disk morphogenesis (41). Very recently, these ectosomes were also found to contain PCARE, WASF3, and several Arp2/3 complex members, and an *ArpC3*$^{-/-}$ mouse model confirmed the Arp2/3-dependent lamellipodium-like actin dynamics mechanism that our results indicate (42). Our data now provide an attractive concept of how ciliary actin may be delivered to the ciliary tip in these actin-regulated processes.

To conclude, we here demonstrate that the protein PCARE, encoded by the former *C2orf71* gene that is mutated in inherited retinal disease, associates with several ciliary proteins as well as those that are involved in the regulation of actin. The membrane expansions that were observed in our cellular coexpression studies, as well as the localization of the endogenous proteins in photoreceptor cells and developing retinal organoids, suggests that PCARE could be involved in the first steps of OS disk neogenesis by the recruitment of an actin dynamics module to the ciliary base and the subsequent transfer of this module to the apical CC region. Most likely, we obtained the identity of only a subset of the components that are part of this machinery. Further analysis of the developing *Pcare*$^{-/-}$ mouse retina by conventional EM would be needed to address the exact defects in OS formation. We did, however, show that we can model the process of ciliary tip expansion in cultured mammalian cells by ectopic expression of PCARE and WASF3, which allows the future evaluation and elucidation of many components that may participate in this critical step in OS development and homeostasis. Finally, our study provides unique insights into the accurate delivery and activation of a multimeric module of actin dynamics regulating proteins, at a tightly restricted suborganellar site of action by a single trafficking molecule: PCARE. This expands the already broad repertoire of the cell to dynamically activate and modulate filamentous actin networks to drive membrane morphogenesis.

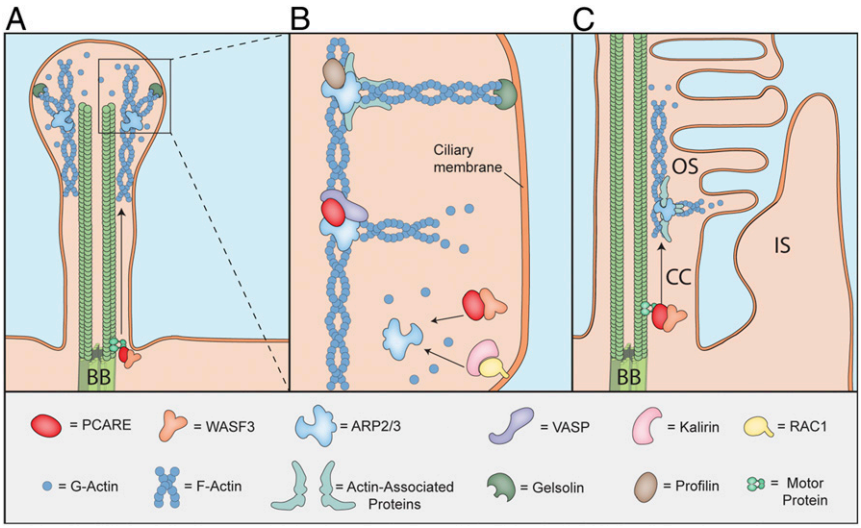

Fig. 6. Proposed model of ciliary membrane modification by PCARE. (*A* and *B*) Expression of exogenous PCARE recruits WASF3 and other modifiers of a dynamic F-actin network assembly to the primary cilium. PCARE and WASF3 might act as actin nucleation promoting factors, by use of their WH2 domain and proline-rich region (44), generating expansion of the ciliary tip. This might be independent or complementary to the action of the Arp2/3 complex (45). Some other potential modifiers are common to the process of lamellipodia formation, such as the Rho-GEF kalirin, an activator of the Rho GTPase Rac1 (46); Rac1, a WAVE complex activator (22); ENA/VASP (VASP) and profilin, both actin elongation factors (47); and the capping protein gelsolin. (*C*) This model may be extrapolated to the photoreceptor cilium, also based on our observations in the developing retinal organoids. We suggest that PCARE is important for the recruitment of actin-associated proteins to the base of the OSs. These proteins may be relevant for the proper expansion of the photoreceptor ciliary membrane that generates new OS disks.

Materials and Methods

Details on DNA constructs, Y2H assay, TAP, cell culture, retinal organoid generation, generation of stable cell lines, siRNA treatment, compound treatments, coimmunoprecipitation, Western blotting, immunofluorescence, animals, in vivo electroporation, EM, and statistical analysis are all provided in *SI Appendix, Supplementary Materials and Methods* and Table S2.

Data Availability. All analyzed datasets are included in the manuscript and *SI Appendix*.

ACKNOWLEDGMENTS. We thank Lisette Hetterschijt, Elisabeth Sehn, and Gabriele B. Stern-Schneider for technical assistance; Drs. Erich Nigg and Nicholas Katsanis for providing expression constructs; Dr. Maxence Nachury for providing IMCD3 Flp-In cells; Dr. Carsten Janke for providing antibodies; Dr. Zhiqian Dong (Case Western Reserve University, CWRU), Dr. Wendy Sun (CWRU), and David Peck (CWRU) for technical help on *Pcare*$^{-/-}$ mouse experiments; and Dr. Thomas Burgoyne for valuable discussion of the EM experiments. This work was funded by the FP7-PEOPLE-2012-ITN program EyeTN, Brussels, Belgium (Grant Agreement 317472) to R.W.J.C.; the Tistou & Charlotte Kerstan Stiftung to M.U.; Fight for Sight and the Wellcome Trust to M.E.C.; the European Community's Seventh Framework FP7/2009 program SYSCILIA (Grant Agreement 241955) to U.W., M.U., and R.R.; the Foundation Fighting Blindness (Program Project Award PPA-0717-0719-RAD) to U.W., M.U., M.E.C., and R.R.; the Netherlands Organization for Scientific Research (NWO Vici Award 865.12.005) to R.R.; and The Netherlands Organization for Health Research and Development (ZonMW TOP Award 91216051) to R.R. and R.W.J.C.

1. D. H. Anderson, S. K. Fisher, R. H. Steinberg, Mammalian cones: Disc shedding, phagocytosis, and renewal. *Invest. Ophthalmol. Vis. Sci.* **17**, 117–133 (1978).
2. S. E. Nilsson, Receptor cell outer segment development and ultrastructure of the disk membranes in the retina of the tadpole (*Rana Pipiens*). *J. Ultrastruct. Res.* **11**, 581–602 (1964).
3. A. F. Goldberg, R. S. Molday, Defective subunit assembly underlies a digenic form of retinitis pigmentosa linked to mutations in peripherin/rds and rom-1. *Proc. Natl. Acad. Sci. U.S.A.* **93**, 13726–13730 (1996).
4. H. May-Simera, K. Nagel-Wolfrum, U. Wolfrum, Cilia–The sensory antennae in the eye. *Prog. Retin. Eye Res.* **60**, 144–180 (2017).
5. R. Roepman, U. Wolfrum, Protein networks and complexes in photoreceptor cilia. *Subcell. Biochem.* **43**, 209–235 (2007).
6. R. W. Young, The renewal of photoreceptor cell outer segments. *J. Cell Biol.* **33**, 61–72 (1967).
7. R. H. Steinberg, S. K. Fisher, D. H. Anderson, Disc morphogenesis in vertebrate photoreceptors. *J. Comp. Neurol.* **190**, 501–508 (1980).
8. T. Burgoyne *et al*., Rod disc renewal occurs by evagination of the ciliary plasma membrane that makes cadherin-based contacts with the inner segment. *Proc. Natl. Acad. Sci. U.S.A.* **112**, 15922–15927 (2015).
9. M. H. Chaitin, B. G. Schneider, M. O. Hall, D. S. Papermaster, Actin in the photoreceptor connecting cilium: Immunocytochemical localization to the site of outer segment disk formation. *J. Cell Biol.* **99**, 239–247 (1984).
10. K. Arikawa, D. S. Williams, Organization of actin filaments and immunocolocalization of alpha-actinin in the connecting cilium of rat photoreceptors. *J. Comp. Neurol.* **288**, 640–646 (1989).
11. D. S. Williams, K. A. Linberg, D. K. Vaughan, R. N. Fariss, S. K. Fisher, Disruption of microfilament organization and deregulation of disk membrane morphogenesis by cytochalasin D in rod and cone photoreceptors. *J. Comp. Neurol.* **272**, 161–176 (1988).
12. R. W. J. Collin *et al*., Mutations in C2ORF71 cause autosomal-recessive retinitis pigmentosa. *Am. J. Hum. Genet.* **86**, 783–788 (2010).
13. D. Y. Nishimura *et al*., Discovery and functional analysis of a retinitis pigmentosa gene, C2ORF71. *Am. J. Hum. Genet.* **86**, 686–695 (2010).
14. L. M. Godsel, D. M. Engman, Flagellar protein localization mediated by a calcium-myristoyl/palmitoyl switch mechanism. *EMBO J.* **18**, 2057–2065 (1999).
15. J. F. Reiter, M. R. Leroux, Genes and molecular pathways underpinning ciliopathies. *Nat. Rev. Mol. Cell Biol.* **18**, 533–547 (2017).
16. S. Suetsugu, H. Miki, T. Takenawa, Identification of two human WAVE/SCAR homologues as general actin regulatory molecules which associate with the Arp2/3 complex. *Biochem. Biophys. Res. Commun.* **260**, 296–302 (1999).
17. S. Eden, R. Rohatgi, A. V. Podtelejnikov, M. Mann, M. W. Kirschner, Mechanism of regulation of WAVE1-induced actin nucleation by Rac1 and Nck. *Nature* **418**, 790–793 (2002).
18. A. Y. Pollitt, R. H. Insall, WASP and SCAR/WAVE proteins: The drivers of actin assembly. *J. Cell Sci.* **122**, 2575–2578 (2009).
19. L. J. Jensen, P. Bork, Biochemistry. Not comparable, but complementary. *Science* **322**, 56–57 (2008).
20. B. M. Kevany, N. Zhang, B. Jastrzebska, K. Palczewski, Animals deficient in C2Orf71, an autosomal recessive retinitis pigmentosa-associated locus, develop severe early-onset retinal degeneration. *Hum. Mol. Genet.* **24**, 2627–2640 (2015).
21. P. Penzes *et al*., An isoform of kalirin, a brain-specific GDP/GTP exchange factor, is enriched in the postsynaptic density fraction. *J. Biol. Chem.* **275**, 6395–6403 (2000).
22. B. Chen *et al*., Rac1 GTPase activates the WAVE regulatory complex through two distinct binding sites. *eLife* **6**, e29795 (2017).
23. S. Bisi *et al*., Membrane and actin dynamics interplay at lamellipodia leading edge. *Curr. Opin. Cell Biol.* **25**, 565–573 (2013).
24. J. Z. Torres, J. J. Miller, P. K. Jackson, High-throughput generation of tagged stable cell lines for proteomic analysis. *Proteomics* **9**, 2888–2891 (2009).
25. S. MacLean-Fletcher, T. D. Pollard, Mechanism of action of cytochalasin B on actin. *Cell* **20**, 329–341 (1980).
26. I. Spector, N. R. Shochet, D. Blasberger, Y. Kashman, Latrunculins—Novel marine macrolides that disrupt microfilament organization and affect cell growth: I. Comparison with cytochalasin D. *Cell Motil. Cytoskeleton* **13**, 127–144 (1989).
27. M. V. Nachury *et al*., A core complex of BBS proteins cooperates with the GTPase Rab8 to promote ciliary membrane biogenesis. *Cell* **129**, 1201–1213 (2007).
28. M. Toriyama *et al*.; University of Washington Center for Mendelian Genomics, The ciliopathy-associated CPLANE proteins direct basal body recruitment of intraflagellar transport machinery. *Nat. Genet.* **48**, 648–656 (2016).
29. A. Michelot, D. G. Drubin, Building distinct actin filament networks in a common cytoplasm. *Curr. Biol.* **21**, R560–R569 (2011).
30. K. Rottner, J. Faix, S. Bogdan, S. Linder, E. Kerkhoff, Actin assembly mechanisms at a glance. *J. Cell Sci.* **130**, 3427–3435 (2017).
31. Z. Chen *et al*., Structure and control of the actin regulatory WAVE complex. *Nature* **468**, 533–538 (2010).
32. K. Djinovic-Carugo, M. Gautel, J. Ylänne, P. Young, The spectrin repeat: A structural platform for cytoskeletal protein assemblies. *FEBS Lett.* **513**, 119–123 (2002).
33. A. F. Goldberg, O. L. Moritz, D. S. Williams, Molecular basis for photoreceptor outer segment architecture. *Prog. Retin. Eye Res.* **55**, 52–81 (2016).
34. G. M. Cammarata, E. A. Bearce, L. A. Lowery, Cytoskeletal social networking in the growth cone: How +TIPs mediate microtubule-actin cross-linking to drive axon outgrowth and guidance. *Cytoskeleton (Hoboken)* **73**, 461–476 (2016).
35. K. J. Carss *et al*.; NIHR-BioResource Rare Diseases Consortium, Comprehensive rare variant analysis via whole-genome sequencing to determine the molecular pathology of inherited retinal disease. *Am. J. Hum. Genet.* **100**, 75–90 (2017).
36. H. H. Arts *et al*., Mutations in the gene encoding the basal body protein RPGRIP1L, a nephrocystin-4 interactor, cause Joubert syndrome. *Nat. Genet.* **39**, 882–888 (2007).
37. A. I. den Hollander *et al*., Mutations in LCA5, encoding the ciliary protein lebercilin, cause Leber congenital amaurosis. *Nat. Genet.* **39**, 889–895 (2007).
38. R. Megaw *et al*., Gelsolin dysfunction causes photoreceptor loss in induced pluripotent cell and animal retinitis pigmentosa models. *Nat. Commun.* **8**, 271 (2017).
39. S. C. Phua *et al*., Dynamic remodeling of membrane composition drives cell cycle through primary cilia excision. *Cell* **168**, 264–279.e15 (2017).
40. A. R. Nager *et al*., An actin network dispatches ciliary GPCRs into extracellular vesicles to modulate signaling. *Cell* **168**, 252–263.e14 (2017).
41. R. Y. Salinas *et al*., Photoreceptor discs form through peripherin-dependent suppression of ciliary ectosome release. *J. Cell Biol.* **216**, 1489–1499 (2017).
42. W. J. Spencer *et al*., Photoreceptor disc membranes are formed through an Arp2/3-dependent lamellipodium-like mechanism. *Proc. Natl. Acad. Sci. U.S.A.* **116**, 27043–27052 (2019).
43. K. Boldt *et al*.; UK10K Rare Diseases Group, An organelle-specific protein landscape identifies novel diseases and molecular mechanisms. *Nat. Commun.* **7**, 11491 (2016).
44. R. Dominguez, The WH2 domain and actin nucleation: Necessary but insufficient. *Trends Biochem. Sci.* **41**, 478–490 (2016).
45. R. D. Mullins, J. A. Heuser, T. D. Pollard, The interaction of Arp2/3 complex with actin: Nucleation, high affinity pointed end capping, and formation of branching networks of filaments. *Proc. Natl. Acad. Sci. U.S.A.* **95**, 6181–6186 (1998).
46. J. H. Wu *et al*., Kalirin promotes neointimal hyperplasia by activating Rac in smooth muscle cells. *Arterioscler. Thromb. Vasc. Biol.* **33**, 702–708 (2013).
47. D. Breitsprecher *et al*., Clustering of VASP actively drives processive, WH2 domain-mediated actin filament elongation. *EMBO J.* **27**, 2943–2954 (2008).